Nitrogen Dioxide Reactions with 46 Atomic Main-Group and Transition Metal Cations in the Gas phase: Room Temperature Kinetics and Periodicities in Reactivity

ARTICLE *in* THE JOURNAL OF PHYSICAL CHEMISTRY A · AUGUST 2012

Impact Factor: 2.69 · DOI: 10.1021/jp304959r

4 AUTHORS:

Michael Jarvis
AB SCIEX
24 PUBLICATIONS **221** CITATIONS
SEE PROFILE

Voislav Blagojevic
Vida Holdings Corp.
42 PUBLICATIONS **705** CITATIONS
SEE PROFILE

Gregory K Koyanagi
York University
58 PUBLICATIONS **1,223** CITATIONS
SEE PROFILE

Diethard K Bohme
York University
422 PUBLICATIONS **8,803** CITATIONS
SEE PROFILE

THE JOURNAL OF PHYSICAL CHEMISTRY A

Article

pubs.acs.org/JPCA

Nitrogen Dioxide Reactions with 46 Atomic Main-Group and Transition Metal Cations in the Gas phase: Room Temperature Kinetics and Periodicities in Reactivity

Michael J. Y. Jarvis, Voislav Blagojevic, Gregory K. Koyanagi, and Diethard K. Bohme*

Department of Chemistry, Centre for Research in Mass Spectrometry and Centre for Research in Earth and Space Science, York University, Toronto, Ontario, Canada, M3J 1P3.

ABSTRACT: Experimental results are reported for the gas-phase room-temperature kinetics of chemical reactions between nitrogen dioxide (NO_2) and 46 atomic main-group and transition metal cations (M^+). Measurements were taken with an inductively-coupled plasma/selected-ion flow tube (ICP/SIFT) tandem mass spectrometer in helium buffer gas at a pressure of 0.35 ± 0.01 Torr and at 295 ± 2 K. The atomic cations were produced at ca. 5500 K in an ICP source and allowed to decay radiatively and to thermalize to room temperature by collisions with Ar and He atoms prior to reaction with NO_2. Measured apparent bimolecular rate coefficients and primary reaction product distributions are reported for all 46 atomic metal cations and these provide an overview of trends across and down the periodic table. Three main types of reactions were observed: O-atom transfer to form either MO^+ or NO^+, electron transfer to form NO_2^+, and addition to form MNO_2^+. Bimolecular O-atom transfer was observed to predominate. Correlations are presented between reaction efficiency and the O-atom affinity of the metal cation and between the prevalence of NO^+ product formation and the electron recombination energy of the product metal oxide cation. Some second-order reactions are evident with metal cations that react inefficiently. Most interesting of these is the formation of the MNO^+ cation with Rh^+ and Pd^+. The higher-order chemistry with NO_2 is very diverse and includes the formation of numerous NO_2 ion clusters and a number of tri- and tetraoxide metal cations. Group 2 metal dioxide cations (CaO_2^+, SrO_2^+, BaO_2^+) exhibit a unique reaction with NO_2 to form $MO(NO)^+$ ions perhaps by NO transfer from NO_2 concurrent with O_2 formation by recombination of a NO_2 and an oxide oxygen.

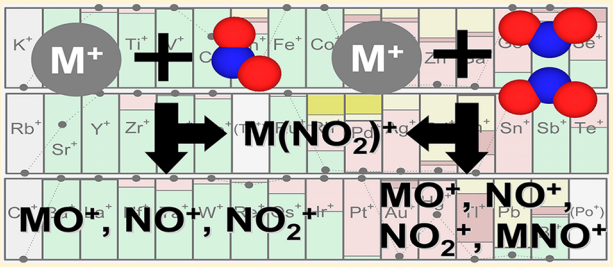

1. INTRODUCTION

In addition to its aeronomic importance as a catalyst in the decomposition of atmospheric ozone,[1,2] nitrogen dioxide (NO_2) is well-known as a major environmental pollutant that is produced as a byproduct of automobile and industrial fuel combustion.[3] As such, the search for efficient and cost-effective methods of treating exhaust gases to remove or reduce nitrogen oxides (NO_x) has been the subject of intense research.[4−6] Very few studies of reactions with NO_2 with atomic metal cations are available in the literature, and this is somewhat surprising given the importance of NO_2. Reactions of Al^+ and Zn^+ were studied some 20 years ago using guided ion beam techniques,[7,8] and NO_2 has been used once as a reagent in the generation of ThO_2^+.[9] Reaction kinetics and product distributions were not measured in these studies. A previous study in our own laboratory of room-temperature reactions of atomic lanthanide cations and NO_2 leading to metal oxide ion formation has been the most extensive of its kind so far.[10] Here we report extensive experimental results for the room-temperature kinetics and product distributions of gas-phase reactions between nitrogen dioxide and 46 atomic main-group and transition metal cations. We also explore the ensuing higher-order chemistry.

2. EXPERIMENTAL METHODS

The experimental results reported herein were obtained using an inductively-coupled plasma/selected-ion flow tube (ICP/SIFT) tandem mass spectrometer, described in detail elsewhere.[11,12] The atomic metal cations were generated in an inductively coupled argon plasma ion source at ca. 5500 K. Solutions containing the metal salt of interest having a concentration of approximately 5 μg L^{-1} were peristaltically pumped via a nebulizer into the plasma. The metal-salt solutions were prepared using atomic spectroscopy standard solutions commercially available from SPEX, Teknolab, J. T. Baker Chemical Co., Fisher Scientific Co., Perkin-Elmer, and Alfa Products. Upon emerging from the ion source, the atomic metal ions were injected through a differentially pumped sampling interface into a quadrupole mass filter and, after mass analysis, introduced through an aspirator-like interface into flowing helium (Linde, 99.98%) carrier gas at 0.35 Torr and 295 ± 2 K. After experiencing about 10^5 collisions with He atoms, the ions were

Special Issue: Peter B. Armentrout Festschrift

Received: May 22, 2012
Revised: August 15, 2012

   dx.doi.org/10.1021/jp304959r | J. Phys. Chem. A XXXX, XXX, XXX−XXX

allowed to react with NO_2 (Linde, 99.5%) added into the flow tube.

The atomic metal ions emerging from the ICP initially have a Boltzmann internal energy distribution characteristic of the plasma temperature of 5500 K. However, these emerging populations are expected to be downgraded in energy during the approximately 20 ms duration before entry into the reaction region in the flow tube. Energy degradation can occur by radiative electronic-state relaxation and by collisional electronic-state relaxation. The latter may occur with argon as the extracted plasma cools upon sampling and then by collisions with He atoms in the flow tube (ca. 4×10^5 collisions) before entry into the reaction region. The extent to which quenching of any electronically excited states of the metal cations that may be formed within the ICP is complete is uncertain and could be inferred only indirectly from the observed decays of primary ion signals. The observed semilogarithmic decays of the fast reacting metal cations were invariably linear for as much as three decades of ion depletion and so were indicative of single-state populations. For the slow reacting metal cations, due to lack of decay, we are unable to make any such conclusions. The large number of collisions with Ar and He between the source and the reaction region should be sufficient to ensure that the atomic lanthanide ions reach a translational temperature equal to the tube temperature of 295 ± 2 K prior to entering the reaction region.

Reactant and product ions were sampled and mass analyzed at the end of the flow tube with a second quadrupole mass filter, and their abundances measured as a function of added reactant. The resulting abundance-versus-reactant profiles provide information about reaction rate coefficients and product-ion distributions. Reaction rate coefficients were determined in the usual manner.[13,14] Primary rate coefficients are determined from the observed semilogarithmic decay of the primary reactant ion intensity using pseudofirst order kinetics and have an estimated accuracy of ±30%.

The NO_2 reagent gas was introduced into the reaction region of the SIFT as a dilute mixture in helium (~17−19%). The NO_2 was obtained commercially from Linde Liquefied Gas and has a nominal purity of 99.5%. In contrast with the vast majority of gaseous reagents that have been studied previously in our laboratory NO_2 has a high propensity toward dimerization, leading to the formation of the N_2O_4 molecule. To obtain an accurate measurement of NO_2 gas flow, measured molecular flow is corrected to take into account dimerization effects according to the procedure that we have developed previously.[10] Although NO_2 exhibits dimerization in the gas handling system, the low pressure of the flow tube (0.35 Torr, with a maximum of 0.1% NO_2 reagent) ensures that there is essentially no dimer present (99.9996% NO_2) at 295 K; we therefore assume that all of the N_2O_4 that enters the flow tube will dissociate before reacting.

3. RESULTS AND DISCUSSION

The gas-phase reactions of 46 atomic main-group and transition metal cations (M^+) with NO_2 were investigated at a helium buffer-gas pressure of 0.35 ± 0.01 Torr and a temperature of 295 ± 2 K. Both the primary and higher-order chemistry was monitored. Rate coefficients (k) for the primary reactions of M^+ ions with NO_2 (both first order and second order in NO_2) were determined by fitting the observed semilogarithmic decay of the reactant ion intensity using pseudo-first-order kinetics. To assess the efficiency (k/k_c) of the reactions studied, the algorithm of the modified variational transition-state/classical trajectory theory developed by Su and Chesnavich[15] was used to calculate collision rate coefficients (k_c). Values of $\alpha(NO_2)$ = 3.02 Å^3 and $\mu_D(NO_2)$ = 0.316 D were adopted for the polarizability and dipole moment, respectively.[16,17]

Figure 1 provides an overview that tracks changes in measured reaction efficiencies and product distributions across and down the periodic table. Measured ion profiles are shown in Figures 2 and 3 for several of the reactions investigated. The solid lines represent kinetic fits to the experimental data. The measured rate

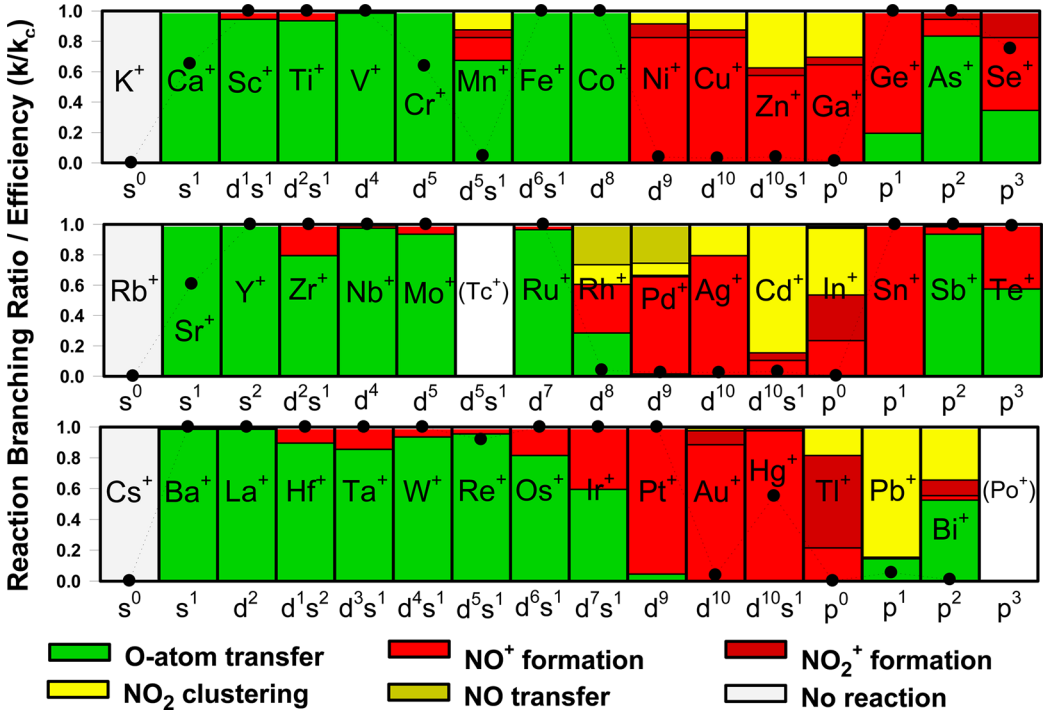

Figure 1. Overview of primary chemistry and room-temperature kinetics for reactions of atomic metal cations with NO_2.

dx.doi.org/10.1021/jp304959r | J. Phys. Chem. A XXXX, XXX, XXX−XXX

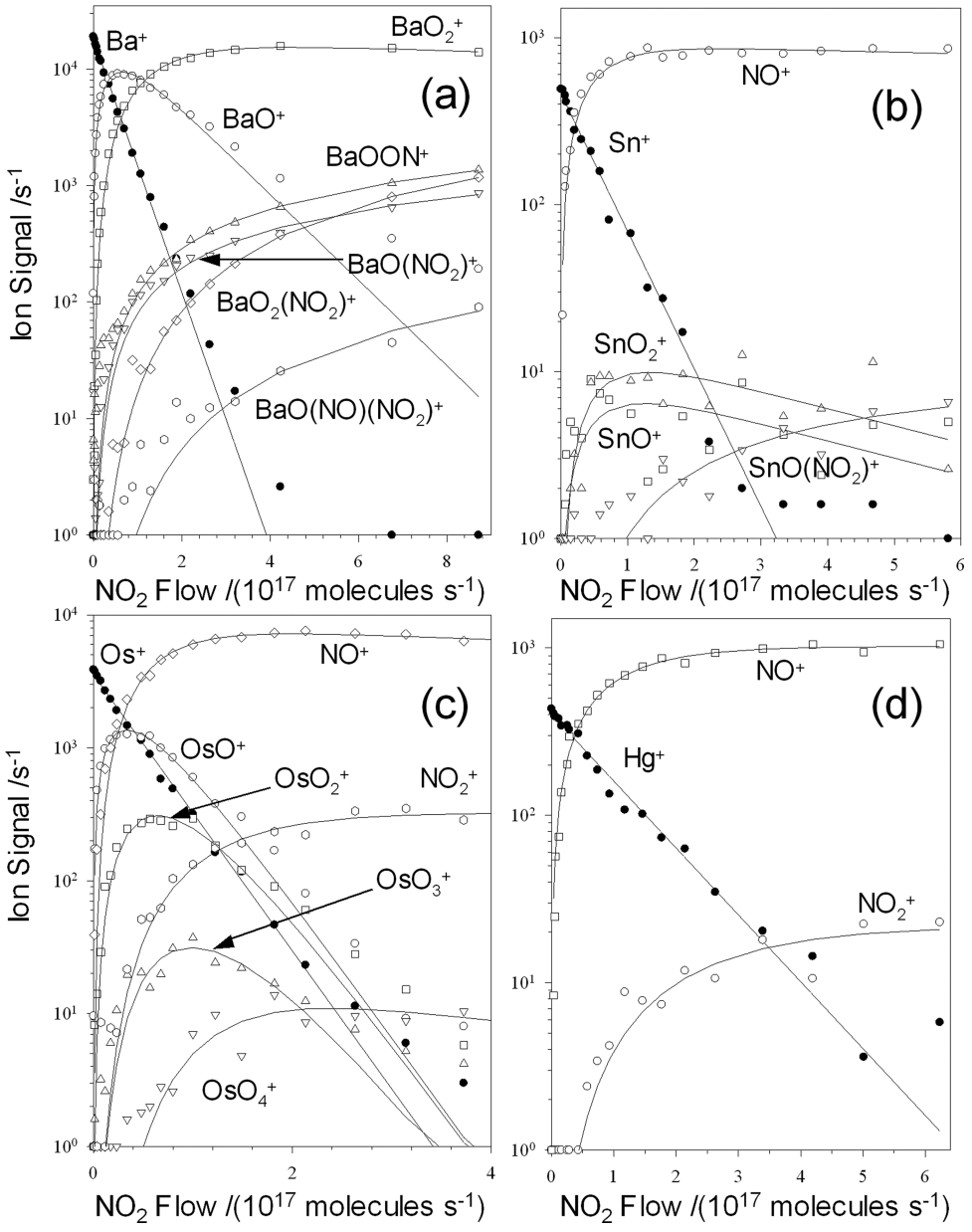

Figure 2. Reaction profiles representative of fast reactions of metal cations with NO_2 first-order in NO_2.

coefficients are summarized in Tables 1 and 2. Table 1 includes fast reactions ($k > 2 \times 10^{-10}$ cm^3 molecule^{-1} s^{-1}) with exothermic bimolecular reaction products, as well as very slow reactions ($k < 10^{-13}$ cm^3 molecule^{-1} s^{-1}) with no exothermic bimolecular reaction products for which no products were observed. Table 2 includes slow reactions (with k between 3×10^{-13} and 3×10^{-11} cm^3 molecule^{-1} s^{-1}) for which bimolecular reaction products are endothermic but product ions were observed. These reactions are deemed to be second order in NO_2. The assessment of the thermodynamics of the formation of reaction products was based on the O-atom affinities of the atomic metal cations (OA) and the ionization energies of the metal atoms (or recombination energies of the atomic metal cations) (IE) given in Table 3. The energy required to remove an O atom from NO_2 in a bimolecular reaction is relatively low, OA(NO) = 72.5 kcal mol^{-1},[18] whereas the energy required to remove an electron is relatively high, IE(NO_2) = 9.59 eV.[18] Second-order chemistry becomes feasible when the intermediate adduct of M^+ and NO_2 encounters a second NO_2 molecule prior to dissociation. The thermodynamics of possible second-order reactions can be examined but, unfortunately, thermodynamic information is not available for many of the possibly second-order product ions that are observed, such as for MNO_2^+ and MNO^+, and neutrals that are not.

Products of both first- and second-order reactions were observed to react further with NO_2 in higher order chemistry. These are summarized in Table 4.

First-Order NO_2 Chemistry: $M^+ + NO_2$. Two main types of reactions can be attributed solely to the first-order reactions of atomic metal cations with NO_2: O-atom transfer resulting in MO^+ or NO^+ formation, depending on the final location of the charge (Figure 2) and electron transfer, resulting in NO_2^+ formation (Figure 2d). Clustering with NO_2, in which the adduct ion is stabilized in third body collisions (Figure 3), can occur either through collisions with helium (first-order in NO_2) or with NO_2 (second-order in NO_2). Although helium is in large excess, stabilization through helium collisions is less efficient due to its

dx.doi.org/10.1021/jp304959r | J. Phys. Chem. A XXXX, XXX, XXX−XXX

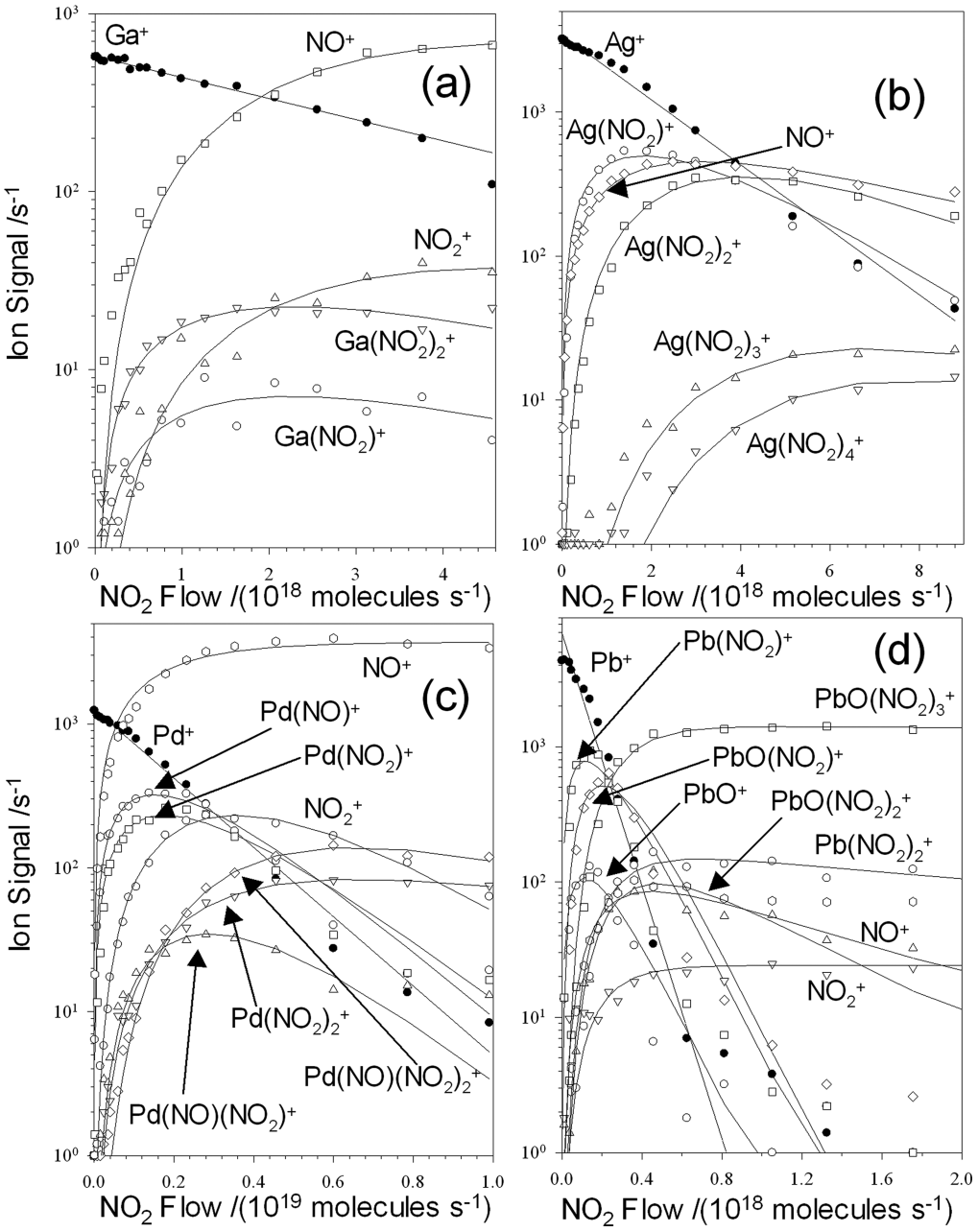

Figure 3. Reaction profiles representative of slow reactions of metal cations with NO_2 second-order in NO_2.

atomic nature and low mass which restrict its ability to accommodate energy, so that stabilization through collisions with NO_2 with its rotational and vibrational modes and higher mass can be expected to be competitive.

First-order O-atom transfer (eqs 1a and 1b) is observed to be very efficient; Ca^+ at 0.43 and Sr^+ at 0.44 exhibit the lowest efficiencies (Table 1). A trend of increasing overall reaction efficiency with increasing O-atom affinity of the atomic metal cation is observed (Figure 4). Bimolecular reactions first-order in NO_2, O-atom and electron transfer, are by far the most efficient reaction pathways exhibited by the atomic metal cations. Only 3 metals have an ionization energy higher than that of NO_2 (9.59 eV),[18] which makes O-atom transfer the only bimolecular reaction pathway available to most atomic metal cations.

$$M^+ + NO_2 \rightarrow MO^+ + NO \quad (1a)$$

$$M^+ + NO_2 \rightarrow MO + NO^+ \quad (1b)$$

The preference of MO^+ vs NO^+ formation correlates quite well with the ionization energy of the metal oxide; a higher IE leads to more prevalent NO^+ (Figure 4). Due to the high exothermicity of many of the O-atom transfer reactions, NO^+ appears as a minor product in many of them. For example, the ionization energies of HfO and TaO are 7.55 and 7.92 eV, well below that of NO at 9.24 eV.[18] The reactions of Hf^+ and Ta^+ with NO_2 show 10% and 14% of NO^+ formation, respectively. The exothermicity of O-atom transfer from NO_2 in both of these examples is in excess of 4 eV ($OA(Hf^+) = 173$, $OA(Ta^+) = 188$ vs $OA(NO) = 72.5$ kcal mol^{-1}),[18] more than enough to form NO^+ by an exothermic reaction in which the reaction exothermicity is deposited in the product metal oxide cation and made available to electron transfer from NO before the products separate. Electron transfer reactions first order in NO_2 are observed with Hg^+, Se^+, and As^+,

dx.doi.org/10.1021/jp304959r | J. Phys. Chem. A XXXX, XXX, XXX−XXX

Table 1. Apparent Bimolecular Rate Coefficients (cm^3 $molecule^{-1}$ s^{-1}), Reaction Efficiencies (k/k_c), and Product Distributions for Reactions of Singly Charged Metal Cations with NO_2 at Room Temperature[a]

metal cation	k	k/k_c	products
K^+	$<10^{-13}$	$<10^{-4}$	none
Ca^+	3.5×10^{-10}	0.43	CaO^+
Sc^+	1.0×10^{-9}	1.1	ScO^+(95%), NO^+(5%)
Ti^+	9.4×10^{-10}	1.0	TiO^+(94%), NO^+(6%)
V^+	8.1×10^{-10}	0.89	VO^+(99%), NO^+(1%)
Cr^+	4.3×10^{-10}	0.47	CrO^+
Fe^+	9.5×10^{-10}	1.1	FeO^+
Co^+	8.1×10^{-10}	0.92	CoO^+
Ge^+	7.1×10^{-10}	0.85	GeO^+(20%), NO^+(80%)
As^+	8.1×10^{-10}	0.96	AsO^+(84%), NO^+(11%), NO_2^+(5%)
Se^+	4.0×10^{-10}	0.48	SeO^+(35%), NO^+(48%), NO_2^+(17%)
Rb^+	$<10^{-13}$	$<10^{-4}$	none
Sr^+	3.5×10^{-10}	0.44	SrO^+
Y^+	7.9×10^{-10}	0.98	YO^+
Zr^+	9.5×10^{-10}	1.2	ZrO^+(80%), NO^+(20%)
Nb^+	9.3×10^{-10}	1.2	NbO^+(98%), NO^+(2%)
Mo^+	5.8×10^{-10}	0.73	MoO^+(94%), NO^+(6%)
Ru^+	8.4×10^{-10}	1.1	RuO^+(97%), NO^+(3%)
Sn^+	6.0×10^{-10}	0.78	SnO^+
Sb^+	8.2×10^{-10}	1.1	SbO^+(94%), NO^+(5%), NO_2^+(1%)
Te^+	5.6×10^{-10}	0.73	TeO^+(58%), NO^+(42%)
Cs^+	$<10^{-13}$	$<10^{-4}$	none
Ba^+	7.9×10^{-10}	1.0	BaO^+(99%), $BaNO_2^+$(1%)
La^+	7.4×10^{-10}	0.97	LaO^+(99%), NO^+(1%)
Hf^+	8.6×10^{-10}	1.2	HfO^+(90%), NO^+(10%)
Ta^+	8.2×10^{-10}	1.1	TaO^+(86%), NO^+(14%)
W^+	1.0×10^{-9}	1.38	WO^+(94%), NO^+(6%)
Re^+	4.8×10^{-10}	0.66	ReO^+(96%), NO^+(4%)
Os^+	7.9×10^{-10}	1.0	OsO^+(82%), NO^+(18%)
Ir^+	7.6×10^{-10}	1.0	IrO^+(60%), NO^+(40%)
Pt^+	7.2×10^{-10}	0.99	PtO^+(5%), NO^+(95%)
Hg^+	2.9×10^{-10}	0.40	NO_2^+(98%), NO^+(2%)

[a]The accuracy of the measured rate coefficients is estimated to be ±30%. O-atom transfer is exothermic in all cases except for the reactions of group 1 metal cations K^+, Rb^+, and Cs^+ that are very endothermic (Table 3) and showed no measurable product ions.

all of which have recombination energies (10.4 eV, 9.75, and 9.81 eV, respectively) that are higher than $IE(NO_2) = 9.59$ eV.[18] In all three cases electron transfer is a minor channel, whereas NO^+ formation is the major channel. NO^+ is formed by O-atom transfer followed by electron transfer, as dissociative electron transfer to form $NO^+ + O$ is endothermic in all three cases.

Second-Order NO_2 Chemistry: $M^+ + 2NO_2$. The second-order NO_2 chemistry appears to be quite diverse. Several different channels attributable solely to second-order reactions have been identified: O-atom transfer, again resulting in both MO^+ and NO^+ as in (3a) and (3b), respectively, MNO^+ formation (3c) and electron transfer (3d), producing NO_2^+. NO_2 adduct formation is at least in part a product of second-order NO_2 reactions 4, but the possible role of helium as the third body cannot be discounted. The first-order reactions have high apparent efficiencies, $k/k_c > 0.4$, but the apparent efficiency of the second-order reactions are much lower $k/k_c < 0.05$. The proposed reaction mechanism is shown in eqs 2 to 4.

$$M^+ + NO_2 \Leftrightarrow [MNO_2^+]^* \quad (2)$$

Table 2. Apparent Bimolecular Rate Coefficients (cm^3 $molecule^{-1}$ s^{-1}), Reaction Efficiencies (k/k_c), and Product Distributions for Second-Order Reactions of Singly Charged Metal Cations with NO_2 at Room Temperature[a]

metal cation	k	k/k_c	products
Mn^+	3.1×10^{-11}	3.4×10^{-2}	MnO^+(68%), NO^+(15%), NO_2^+(5%), $MnNO_2^+$(12%)
Ni^+	2.2×10^{-11}	2.4×10^{-2}	NO^+(83%), NO_2^+(9%), $NiNO_2^+$(8%)
Cu^+	1.8×10^{-11}	2.1×10^{-2}	NO^+(83%), NO_2^+(5%), $CuNO_2^+$(12%)
Zn^+	2.2×10^{-11}	2.5×10^{-2}	NO^+(58%), NO_2^+(5%), $ZnNO_2^+$(37%)
Ga^+	6.3×10^{-12}	7.4×10^{-3}	NO^+(65%), NO_2^+(5%), $GaNO_2^+$(30%)
Rh^+	2.1×10^{-11}	2.6×10^{-2}	RhO^+(29%), NO^+(32%), $RhNO_2^+$(13%), $RhNO^+$(26%)
Pd^+	1.3×10^{-11}	1.6×10^{-2}	PdO^+(2%), NO^+(64%), NO_2^+(1%), $PdNO_2^+$(8%), $PdNO^+$(25%)
Ag^+	1.2×10^{-11}	1.5×10^{-2}	$Ag(NO_2)^+$(20%), NO^+(80%)
Cd^+	1.6×10^{-11}	2.1×10^{-2}	NO^+(11%), NO_2^+(5%), $CdNO_2^+$(84%)
In^+	1.2×10^{-12}	1.5×10^{-3}	NO^+(25%), NO_2^+(30%), $InNO_2^+$(45%)
Au^+	1.7×10^{-11}	2.4×10^{-2}	NO^+(89%), NO_2^+(9%), $AuNO_2^+$(2%)
Tl^+	3×10^{-13}	5×10^{-4}	NO^+(22%), NO_2^+(60%), $TlNO_2^+$(18%)
Pb^+	2.7×10^{-11}	3.7×10^{-2}	PbO+(15%),NO_2^+(1%), $PbNO_2^+$(84%)
Bi^+	4.6×10^{-12}	6.2×10^{-3}	BiO+(53%), NO^+(3%), NO_2^+(10%), $BiNO_2^+$(34%)

[a]The accuracy of the measured rate coefficients is estimated to be ±30%.

Table 3. O-Atom Affinities ($D_0(M^+-O)$, kcal mol^{-1}) and Ionization Energies (IE(M),[18] eV) for Fourth-, Fifth-, and Sixth-Row Atomic Cations

M^+	$OA(M^+)$	IE(M)	M^+	$OA(M^+)$	IE(M)	M^+	$OA(M^+)$	IE(M)
K^+	3[a]	4.34	Rb^+	7[a]	4.18	Cs^+	14[a]	3.89
Ca^+	77.2[a]	6.11	Sr^+	71.4[a]	5.70	Ba^+	92.8[a]	5.21
Sc^+	164.6 ± 1.4[b]	6.56	Y^+	167.0 ± 4.2[c]	6.22	La^+	206 ± 4[e]	5.58
Ti^+	158.6 ± 1.6[b]	6.83	Zr^+	178.9 ± 2.5[c]	6.63	Hf^+	173 ± 5[a]	6.83
V^+	134.9 ± 3.5[b]	6.75	Nb^+	164.4 ± 2.5[c]	6.76	Ta^+	188 ± 15[a]	7.89
Cr^+	85.8 ± 2.8[b]	6.77	Mo^+	116.7 ± 0.5[c]	7.09	W^+	166 ± 10[j]	7.98
Mn^+	68.0 ± 3.0[b]	7.43	Tc^+		7.28	Re^+	115 ± 15[f]	7.88
Fe^+	80.0 ± 1.4[b]	7.90	Ru^+	87.9 ± 1.2[d]	7.36	Os^+	100 ± 12[g]	8.7
Co^+	74.9 ± 1.2[b]	7.88	Rh^+	69.6 ± 1.4[d]	7.46	Ir^+	107 ± 10[k]	9.1
Ni^+	63.2 ± 1.2[b]	7.64	Pd^+	33.7 ± 2.5[d]	8.34	Pt^+	77[h]	9.0
Cu^+	37.4 ± 3.5[b]	7.73	Ag^+	28.4 ± 1.2[d]	7.58	Au^+		9.23
Zn^+	38.5 ± 1.2[b]	9.39	Cd^+		8.99	Hg^+		10.44
Ga^+	5.6[a]	6.00	In^+		5.79	Tl^+		6.11
Ge^+	81.8[a]	7.90	Sn^+	75.1[a]	7.34	Pb^+	53.2[a]	7.42
As^+	147 ± 2[i]	9.82	Sb^+		8.64	Bi^+	41.6[a]	7.29
Se^+	92[i]	9.75	Te^+	96.6[a]	9.01	Po^+		8.42

[a]Reference 19. [b]Reference 20. [c]Reference 21. [d]Reference 22. [e]Reference 23. [f]Reference 24. [g]Reference 25. [h]Reference 26. [i]Reference 27. [j]Reference 28. [k]Reference 29.

$$[MNO_2^+]^* + NO_2 \rightarrow MO^+ + (2N, 3O) \quad (3a)$$

$$\rightarrow NO^+ + (M, N, 3O) \quad (3b)$$

$$\rightarrow MNO^+ + (N, 3O) \quad (3c)$$

$$\rightarrow NO_2^+ + (M, N, 2O) \quad (3d)$$

$$\rightarrow MNO_2^+ + (NO_2)^* \quad (4)$$

Second-order reactions are preceded by the formation of an intermediate $[MNO_2^+]^*$ complex according to eq 2. This is the rate determining step and the source of the low apparent

dx.doi.org/10.1021/jp304959r | J. Phys. Chem. A XXXX, XXX, XXX−XXX

Table 4. Higher-Order Products Observed in Sequential Reactions with NO_2 of Ions Produced by First- or Second-Order Reactions of Metal Cations with NO_2 (Those Listed in Tables 1 and 2)

metal cation	higher-order products
Ca^+	CaO_2^+, $CaO(NO)^+$, $CaO_2(NO)^+$, $CaO_{1,2}(NO)(NO_2)^+$
Sc^+	ScO_{2-3}^+, $ScO(NO)^+$, $ScO(NO_2)^+$, NO^+
Ti^+	TiO_{2-3}^+, $TiO_2(NO)^+$, $TiO_2(NO_2)^+$, $TiO_2(NO)(NO_2)^+$, NO^+, NO_2^+
V^+	VO_2^+, NO^+, NO_2^+
Cr^+	CrO_2^+, NO^+
Mn^+	$MnO(NO_2)^+$, $Mn(NO_2)_2^+$
Fe^+	NO^+, NO_2^+
Co^+	NO^+, NO_2^+
Ni^+	$NO(NO_2)^+$, $(NO_2)_2^+$
Cu^+	$NO(NO_2)^+$, $(NO_2)_2^+$
Zn^+	$NO(NO_2)^+$, $(NO_2)_2^+$
Ga^+	$Ga(NO_2)_2^+$
Ge^+	none
As^+	none
Se^+	SeO_2^+, NO_2^+
Sr^+	SrO_2^+, $SrO_{1,2}(NO)^+$, $SrO_2(NO_2)^+$
Y^+	YO_2^+, $YO_{1,2}(NO)^+$, $YO_{1,2}(NO)(NO_2)^+$, NO^+, NO_2^+
Zr^+	ZrO_{2-3}^+, $ZrO_2(NO)^+$, $ZrO_2(NO)(NO_2)^+$, NO^+, NO_2^+
Nb^+	NbO_2^+, $NbO_2(NO_2)^+$, NO^+, NO_2^+
Mo^+	MoO_2^+, NO^+
Ru^+	RuO_2^+, NO^+
Rh^+	$RhO(NO_2)^+$, $Rh(NO)(NO_2)^+$, NO^+, NO_2^+
Pd^+	$Pd(NO)(NO_2)_{1,2}^+$, $Pd(NO_2)_2^+$, NO^+, NO_2^+
Ag^+	$Ag(NO_2)_{2-4}^+$
Cd^+	NO^+, NO_2^+
In^+	$In(NO_2)_2^+$, NO^+, NO_2^+
Sn^+	SnO_2^+, NO^+
Sb^+	none
Te^+	NO_2^+
Ba^+	BaO_2^+, $BaO(NO_2)^+$, $BaO(NO)^+$, $BaO_2(NO_2)^+$, $BaO(NO)(NO_2)^+$
La^+	LaO_2^+, $LaO(NO_2)^+$
Hf^+	HfO_2^+, HfO_3^+, $HfO_{1-2}(NO_2)^+$, $HfO_{1-2}(NO_2)_2^+$, NO^+, NO_2^+
Ta^+	TaO_2^+, NO^+, NO_2^+
W^+	WO_{2-3}^+, NO^+, NO_2^+
Re^+	ReO_{2-4}^+, NO^+, NO_2^+
Os^+	OsO_{2-4}^+, NO^+, NO_2^+
Ir^+	IrO_2^+, NO^+
Pt^+	NO^+, NO_2^+
Au^+	$Au(NO_2)_{2,3}^+$
Hg^+	none
Tl^+	$Tl(NO_2)_2^+$
Pb^+	$PbO(NO_2)_{1-3}^+$, $Pb(NO_2)_{2-3}^+$, NO^+, NO_2^+
Bi^+	$BiO(NO_2)_{1-4}^+$, $Bi(NO_2)_{2-4}^+$, $BiO_2(NO_2)_{2-4}^+$

efficiency, as this complex needs to survive long enough to collide with another NO_2 molecule. Once a collision with the second NO_2 molecule occurs, the reaction likely proceeds efficiently along one of the channels discussed previously (eqs 3a–3d). Alternatively, quenching of the intermediate $[MNO_2^+]^*$ complex is also possible, creating the NO_2 adduct and rotationally and vibrationally excited NO_2.

Two possibilities for neutral products produced in eq 3a are $NO + NO_2$ and $N_2O + O_2$. Although the enthalpy of formation for $N_2O + O_2$ is somewhat lower than that for $NO + NO_2$, 19.6 vs 29.5 kcal mol^{-1},[18] NO^+ is commonly observed in conjunction with MO^+. Therefore it is again likely that, similar to what is observed for first-order reactions, the reaction exothermicity is deposited in the product metal oxide cation and made available to electron transfer from NO before the products separate. Only Pd^+ and Rh^+ exhibit MNO^+ formation (eq 3c) in which the neutral (N, 3O) product has two possible outcomes, NO_3 and $NO + O_2$. The enthalpy difference between them is small and favors NO_3 formation by 4.6 kcal mol^{-1} (the enthalpies of formation are 17.0 and 21.6 kcal mol^{-1}, respectively)[18] which also should be kinetically favored as it requires less bond redisposition.

There is some doubt regarding the veracity of the second-order electron transfer for some of the metal cation reactions. Second-order reactions have low apparent efficiencies, so it is possible that apparently slow NO_2^+ formation is the product of electron transfer from a small amount of excited metal cation or an isobaric interference (oxide, nitride, or carbide of another metal or an ICP matrix ion). In^+ and Tl^+ both exhibit significant electron transfer but have low recombination energies (5.8 and 6.1 eV, respectively).[18] The energy gap between the IE of In and Tl and that of NO_2 is approximately 3.5 eV.

Higher Order Reactions with NO_2. The chemistry resulting from further reactions of the products of first- and second-order reactions with NO_2 is quite diverse and extensive. Metal oxides are the most reactive class of products, whereas other species primarily undergo clustering with NO_2. Metal oxide cations, MO^+, undergo all the same reactions with NO_2 that the bare metal cation does. Some of the metal oxides are formed in an excited state and there is little time for these to be quenched before encountering another NO_2 and electron transfer to form NO_2^+ is quite common. O-atom transfer, leading to MO_2^+ or NO^+ formation, is also pervasive and NO^+ formation is generally favored over MO_2^+. NO_2 clustering of up to four molecules of NO_2 is also observed. A full list of high order products is given in Table 4.

The extent of O-atom transfer is dependent on the MO^+ vs NO^+ product distribution. Tri- and tetraoxides are observed only with early (ScO_3^+, TiO_3^+, ZrO_3^+, NbO_3^+, HfO_3^+) and midsixth row transition metals (WO_3^+, $ReO_{3,4}^+$, $OsO_{3,4}^+$). NO^+ is usually observed as a concomitant product. Calcium, strontium, and barium all exhibit an unusual $MO(NO)^+$ product that appears to be the result of the reaction $MO_2^+ + NO_2$ (Figure 2a). A likely mechanism for this reaction would involve NO transfer from NO_2 and recombination of an oxygen from both MO_2^+ and NO_2 to form O_2. Because this product is observed only with group 2 metal dioxide cations, it is possible that there is something about the group 2 MO_2^+ ion geometries that makes the NO transfer and oxygen recombination especially favorable.

■ CONCLUSIONS

The chemistry of atomic metal cations with NO_2 at room temperature is dominated by O-atom transfer, producing either MO^+ or NO^+ cations. The distribution of charge between MO and NO (leading to $MO^+ + NO$ or $MO + NO^+$) is dependent on the ionization energy of MO and a high exothermicity of O-atom transfer can result in NO^+ formation when IE(MO) is lower than IE(NO). The reaction efficiency generally increases with the O-atom affinity of the atomic metal cation, indicating the decisive role of M–O bond formation in bimolecular reactions with NO_2. Fast electron transfer is observed as the only channel with Hg^+ and as minor channels with Se^+ and As^+. Slow O-atom transfer second-order in NO_2 also appears to be possible, producing MO^+ or NO^+, generally in competition with NO_2 addition. Palladium

dx.doi.org/10.1021/jp304959r | J. Phys. Chem. A XXXX, XXX, XXX–XXX

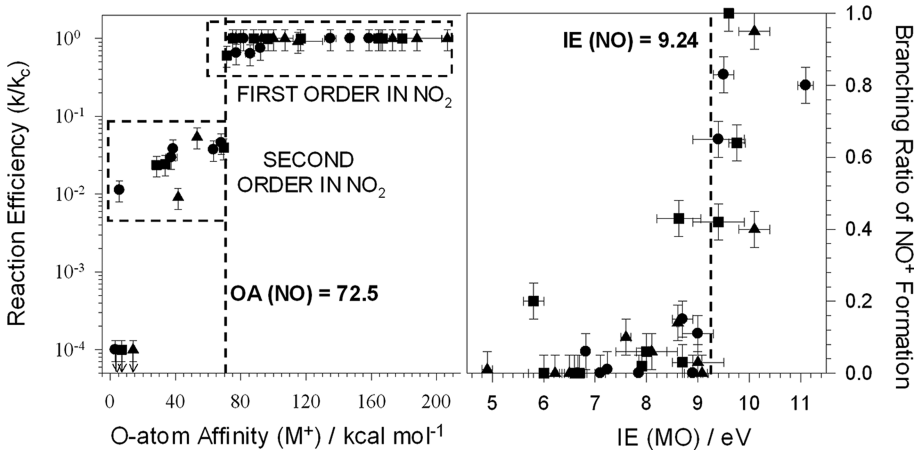

Figure 4. Correlations between reaction efficiency and the O-atom affinity of the metal cation (left) and between primary NO^+ formation and the ionization energy of the metal oxide (right). Circles represent period 4, squares period 5, and triangles period 6 cations. Metal oxide ionization energies are from ref 15 and are not available for all elements (Sc, Cu, Zn, and Se in period 4; Ag, Cd, and Sb in period 5; Re, Os, Au, Hg, and Tl in period 6).

and rhodium cations exhibit a unique second-order reaction producing MNO^+ and either NO_3 or NO + O_2.

The higher order NO_2 chemistry is very rich. Formation of oxides up to tetraoxides and multiple NO_2 clusters is observed. A special highlight is an unusual $MO(NO)^+$ product formed in the reaction of MO_2^+ and NO_2 (M = Ca, Sr, Ba). It is possible that group 2 metal dioxide MO_2^+ cations have special geometric advantage that allows such a reaction, concomitant NO transfer and O_2 recombination, possible.

AUTHOR INFORMATION

Corresponding Author

*E-mail: dkbohme@yorku.ca.

Notes

The authors declare no competing financial interest.

ACKNOWLEDGMENTS

Continued financial support from the Natural Sciences and Engineering Research Council of Canada is greatly appreciated. As holder of a Canada Research Chair in Physical Chemistry, D.K.B. thanks the contributions of the Canada Research Chair Program to this research.

REFERENCES

(1) Rowland, F. S.; Molina, M. J. *Rev. Geophys. Space Ge.* **1975**, *13*, 1−35.
(2) Elliott, S.; Rowland, F. S. *J. Chem. Educ.* **1987**, *64*, 387−391.
(3) Katz, M. *Can. J. Chem. Eng.* **1970**, *48*, 3−11.
(4) Garin, F. *Appl. Catal. A-Gen.* **2001**, *222*, 183−219.
(5) Garin, F. *Catal. Today* **2004**, *89*, 255−268.
(6) Nakatsuji, T.; Komppa, V. *Catal. Today* **2002**, *75*, 407−412.
(7) Clemmer, D. E.; Weber, M. E.; Armentrout, P. B. *J. Phys. Chem.* **1992**, *96*, 10888−10893.
(8) Clemmer, D. E.; Dalleska, N. F.; Armentrout, P. B. *J. Chem. Phys.* **1991**, *95*, 7263−7268.
(9) Cornehl, H. H.; Wesendrup, R.; Diefenbach, M.; Schwarz, H. *Chem.−Eur. J.* **1997**, *3*, 1083−1090.
(10) Jarvis, M. J. Y.; Blagojevic, V.; Koyanagi, G. K.; Bohme, D. K. *Phys. Chem. Chem. Phys.* **2010**, *12*, 4852−4862.
(11) Koyanagi, G. K.; Baranov, V. I.; Tanner, S. D.; Bohme, D. K. *J. Anal. At. Spectrom.* **2000**, *15*, 1207−1210.
(12) Koyanagi, G. K.; Lavrov, V. V.; Baranov, V. I.; Bandura, D.; Tanner, S.; McLaren, J. W.; Bohme, D. K. *Int. J. Mass Spectrom.* **2000**, *194*, L1−L5.
(13) Mackay, G. I.; Vlachos, G. D.; Bohme, D. K.; Schiff, H. I. *Int. J. Mass Spectrom. Ion Phys.* **1980**, *36*, 259−270.
(14) Raksit, A. B.; Bohme, D. K. *Int. J. Mass Spectrom. Ion Processes* **1983/84**, *55*, 69−82.
(15) Su, T.; Chesnavich, W. J. *J. Chem. Phys.* **1982**, *76*, 5183−5185.
(16) Maryott, A. A.; Buckley, F. *U. S. National Bureau of Standards Circular No. 537*; National Bureau of Standards: Washington, DC, 1953
(17) Nelson, R. D.; Lide, D. R.; Maryott, A. A. *Selected Values of Electric Dipole Moments for Molecules in the Gas Phase.* National Bureau of Standards Reference Data Series 10; National Bureau of Standards: Washington, DC, 1967
(18) Linstrom, P. J., Mallard, W. G., Eds. *NIST Chemistry WebBook, NIST Standard Reference Database Number 69*; National Institute of Standards and Technology: Gaithersburg, MD; http://webbook.nist.gov (retrieved August 18, 2011)
(19) Lias, S. G.; Bartmess, J. E.; Liebman, J. F.; Holmes, J. L.; Levin, R. D.; Mallard, W. G. *J. Phys. Chem. Ref. Data* **1988**, *17*, 861.
(20) Freiser, B. S., Ed. *Organnometallic Ion Chemistry*; Kluwer: Dordrecht, The Netherlands, 1996.
(21) Sievers, M. R.; Chen, Y.-M.; Armentrout, P. B. *J. Chem. Phys.* **1996**, *105*, 6322−6333.
(22) Chen, Y.-M.; Armentrout, P. B. *J. Chem. Phys.* **1995**, *103*, 618−625.
(23) Clemmer, D. E.; Dalleska, N. F.; Armentrout, P. B. *Chem. Phys. Lett.* **1992**, *190*, 259−265.
(24) Beyer, M. D. *Dissertation*, Technical University Munchen, 1996.
(25) Irikura, K. K.; Beauchamp, J. L. *J. Am. Chem. Soc.* **1989**, *111*, 75−85.
(26) Pavlov, M.; Blomberg, M. R. A.; Siegbahn, P. E. M.; Wesendrup, R.; Heinemann, C.; Schwarz, H. *J. Phys. Chem. A* **1997**, *101*, 1567−1579.
(27) Lavrov, V. V.; Blagojevic, V.; Koyanagi, G. K.; Orlova, G.; Bohme, D. K. *J. Phys. Chem. A* **2004**, *108*, 5610−5624.
(28) Blagojevic, V.; Koyanagi, G. K.; Lavrov, V. V.; Orlova, G.; Bohme, D. K. *Chem. Phys. Lett.* **2004**, *389*, 303−308.
(29) Calculated using $D(Ir-O) = 84 \pm 5$ kcal mol^{-1} from: Drowart, J.; Goldfinger, P. *Angew. Chem., Int. Ed.* **1967**, *6*, 581−596.